Ion beam mixing of Al-Ti bilayers
by Nancy Lynn Charles

A thesis submitted in partial fulfillment of the requirements for the degree of Master of Science in Physics
Montana State University
© Copyright by Nancy Lynn Charles (1992)

Abstract:
Titanium-aluminum alloys are of much interest to the scientific community as light-weight, strong materials. Understanding how the different compounds and phases are formed allows the improvement and creation of new alloys with improved performance properties. Ion Beam Mixing is a method of compound formation which yields some very different results from thermal annealing, with the possibility of forming new and novel phases of the alloy. Thin bilayer films of Al and Ti are ion mixed with an argon ion beam and analyzed with Rutherford Backscattering Spectrometry. This analysis technique yields information about the sample composition as a function of depth without damaging the sample. The analysis can show phase formation, if present, and the shift in composition of the elements at the interface of the bilayer due to the mixing. This change in elemental composition at the interface can be measured and represented as the mixing rate which can be compared with standard models for the different mechanisms of ion beam mixing. The models of ion mixing are based on the mass of the ions and sample atoms, the energies involved in the mixing process and the thermodynamic properties of materials being mixed. It was found that the ion beam mixing of A-Ti bilayers did not result in significant phase formation for ion doses up to 1x10 16cm-2 The two theoretical models of the ion mixing mechanisms did not yield any useful information about the mixing process since both predict the same result for this system, however, mixing was observed and the mixing rate was similar to that obtained with xenon ions.

ION BEAM MIXING OF

AL-TI BILAYERS

by

Nancy Lynn Charles

A thesis submitted in partial fulfillment
of the requirements for the degree

of

Master of Science

in

Physics

MONTANA STATE UNIVERSITY
Bozeman, Montana

May 1992

N378
C5769

APPROVAL

of a thesis submitted by

Nancy Lynn Charles

This thesis has been read by each member of the thesis committee and has been found to be satisfactory regarding content, English usage, format, citations, bibliographic style, and consistency and is ready for submission to the College of Graduate Studies.

5/12/92
Date

Richard J. Smith
Chairman, Graduate Committee

Approved for the Major Department

5-12-92
Date

Head, Major Department

Approved for the College of Graduate Studies

May 18, 1992
Date

Henry L Parsons
Graduate Dean

STATEMENT OF PERMISSION TO USE

In presenting this thesis in partial fulfillment of the requirements for a Master's degree at Montana State University, I agree that the Library shall make it available to borrowers under rules of the Library. Brief quotations from this thesis are allowable without special permission, provided that accurate acknowledgment of source is made.

Permission for extensive quotation from or reproduction of this thesis may be granted by my major professor, or in his absence, by the Dean of Libraries when, in the opinion of either, the proposed use of the material is for scholarly purposes. Any copying or use of the material in this thesis for financial gain shall not be allowed without my written permission.

Signature Nancy L. Clarke

Date 12 May 1992

ACKNOWLEDGMENTS

I would like to give a special thanks to Norman Williams and Erik Andersen for their technical advice and support. The advice and collaboration of Adli Saleh and V. Shutthanandan are also greatly appreciated. A very warm thank you goes to Randy Equall for his support and the use of his computer.

Finally, I would like to thank my advisor Dr. Richard Smith for all his enthusiasm, patience and advice.

TABLE OF CONTENTS

Page

1. INTRODUCTION 1

2. ANALYSIS AND EXPERIMENTAL TECHNIQUES 3

   Rutherford Backscattering Spectrometry 3
   Ion Beam Mixing 8

3. SAMPLE PREPARATION 10

4. THEORY 12

   Mechanisms of Ion Beam Mixing 12
   Quantifying the Amount of Mixing 13
   Models of Mixing Mechanisms 14
   Thermodynamic Considerations 16

5. RESULTS AND ANALYSIS 18

   Sample Analysis and Normalization 18
   Experimental Results 22
   Phase Formation by Ion Beam Mixing 25
   Discussion of an Earlier Sample 31

6. CONCLUSION 36

REFERENCES 38

LIST OF TABLES

Table Page

1. Heats of formation for Al-Ti phases 17
2. Experimental and modeled mixing rates of Al-Ti from Ar^+ and Xe^+ mixing 24
3. Table of parameters used to calculate the theoretical mixing rates for Al-Ti 24
4. Percentage of Al sputtered away as a function of dose 34

LIST OF FIGURES

Figure Page

1. Schematic of apparatus used for Rutherford Backscattering Spectrometry 3
2. Simple schematic of Rutherford Backscattering Spectrometry 4
3. Sample target, real and ideal RBS spectra 6
4. Schematic of apparatus used for ion beam mixing 9
5. Finding ΔE for calculating the variance from the RBS spectrum 14
6. RBS spectrum of unmixed sample and ideal simulation 18
7. RBS spectrum of unmixed sample and fitted simulation 19
8. Demonstration of points used to find ΔE 21
9. Plot of variance versus dose 22
10. RBS spectrum of a thermally annealed Al-Ti bilayer 26
11. Overlay of the RBS spectra for various doses 27
12. Simulation of the RBS spectra for the Al-Ti phases 28
13. Enlargement of Al peak at two different doses to show possible phase formation . 29
14. RBS spectrum of a mixed sample and fitted simulation 30
15. Plot of variance versus dose for a previous sample 32
16. Overlay of the RBS spectra for various doses for a previous sample 33

ABSTRACT

Titanium-aluminum alloys are of much interest to the scientific community as light-weight, strong materials. Understanding how the different compounds and phases are formed allows the improvement and creation of new alloys with improved performance properties. Ion Beam Mixing is a method of compound formation which yields some very different results from thermal annealing, with the possibility of forming new and novel phases of the alloy. Thin bilayer films of Al and Ti are ion mixed with an argon ion beam and analyzed with Rutherford Backscattering Spectrometry. This analysis technique yields information about the sample composition as a function of depth without damaging the sample. The analysis can show phase formation, if present, and the shift in composition of the elements at the interface of the bilayer due to the mixing. This change in elemental composition at the interface can be measured and represented as the mixing rate which can be compared with standard models for the different mechanisms of ion beam mixing. The models of ion mixing are based on the mass of the ions and sample atoms, the energies involved in the mixing process and the thermodynamic properties of materials being mixed. It was found that the ion beam mixing of Al-Ti bilayers did not result in significant phase formation for ion doses up to $1x10^{16}cm^{-2}$. The two theoretical models of the ion mixing mechanisms did not yield any useful information about the mixing process since both predict the same result for this system, however, mixing was observed and the mixing rate was similar to that obtained with xenon ions.

CHAPTER 1

INTRODUCTION

There is much interest in titanium aluminides as structural materials. Their relatively low density and elevated temperature properties are especially attractive to the aerospace industry for engine and airframe components[1], to the medical community for making artificial joints and bones[2] and to many others interested in lightweight, strong materials. Understanding these alloys, how the elements Ti and Al react, how to make new phases with new properties, learning to control the growth and phase formation of the desired alloy, is critical for improving their usefulness. One of the ways in which alloys can be formed is by ion beam mixing. Ion beam mixing is the mixing of a target, usually comprised of elemental layers, at the atomic level by accelerating high energy ions onto the target. The incident ions are usually inert (argon, krypton, xenon, etc.) so that they do not interact with the target. While this method is limited to the surface of an object, it is useful in its mixing efficiency and its occasional ability to cause novel and thermodynamically unfavorable phases to form in the target.

Ion beam mixing was first discovered by Van der Weg et al. in 1973[3] when palladium silicide formed due to Ar ion irradiation of Pd films on Si substrates. The novelty was that for every incident Ar ion more than 100 atoms of Pd and Si were mixed, and so could not be explained by simple ballistic recoil of the target atoms. In the nearly 20 years since then much data has been accumulated for many systems, including bilayer films, multilayer films and thin film markers embedded in a substrate. Much of the ion mixing described in the literature has been done with Xe ions since Xe

is relatively heavy and inert. There is some interest in the relationship between the incident ion mass and the amount of mixing produced in the sample.

This work presents a study of Al-Ti bilayer films mixed with Ar ions. Does ion beam mixing with Ar^+ at room temperature result in phase formation? If so, is it possible to predict which phases are formed based on thermal annealing results or the thermodynamic properties of the system? If phases are not formed by ion beam mixing for this bilayer, can the mixing be described by various mixing mechanism models? The models which quantify the mixing are discussed and computed for this bilayer system. A comparison between mixing of these bilayers with Ar ions and mixing of the same with Xe ions as found in the literature is also addressed. Thermodynamic considerations are also discussed, as well as their possible role in enhancing or inhibiting mixing and phase formation of Al-Ti compounds due to ion beam mixing with Ar.

CHAPTER 2

ANALYSIS AND EXPERIMENTAL TECHNIQUES

Rutherford Backscattering Spectrometry

Rutherford Backscattering Spectrometry (RBS) is a powerful technique that can yield an abundance of information about a sample and is used extensively in this analysis. The apparatus used for this technique is shown below in Figure 1 and consists of a 2MV Van de Graaff type AK model N positive-ion accelerator, a bending magnet and the chamber and goniometer for mounting the sample to be analyzed.

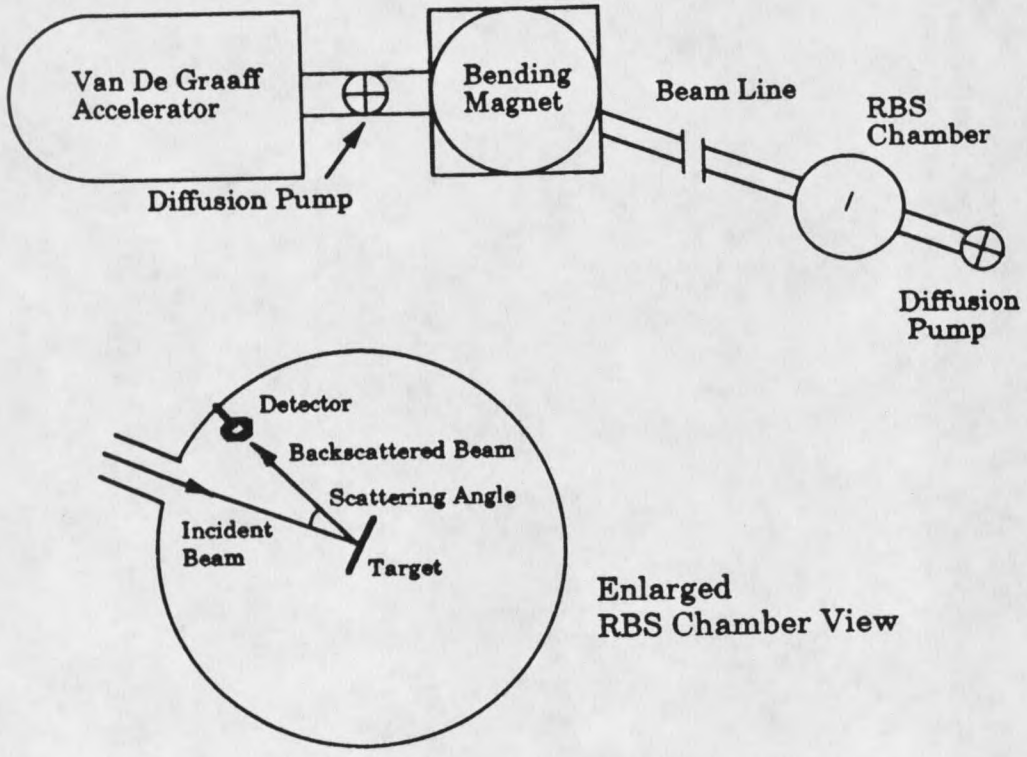


Figure 1. Schematic of apparatus used for Rutherford Backscattering Spectrometry

The backscattering technique consists of creating high energy (~1.8 MeV, in this case) helium ions in the Van de Graaff accelerator, collimating them into a focused beam, bending the beam through the magnet which selects only the ions with the chosen energy, and centering the beam on the sample target to be analyzed in the chamber. The light helium ions backscatter off the atoms of the target and are detected by a solid-state detector which is in the plane of the incident beam and sample normal direction and at a fixed angle with respect to the beam and the target. A simple diagram of this geometry is shown in Figure 2.

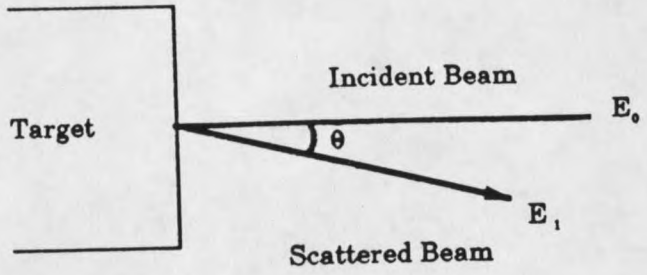


Figure 2. Simple schematic of Rutherford Backscattering Spectrometry

The detector is connected through a pre-amp and amplifier to a Multichannel Analyzer (MCA), which records the number of backscattered helium ions detected as a function of their scattered energy. The energy with which the helium ions backscatter, E_1, is a function of their incident energy, E_0, the ratio of the He ion mass to the target atom mass, and the scattering angle. The dependence on the mass ratios and the scattering angle has been defined as the kinematic factor[4],

$$K = \frac{E_1}{E_0} = \left\{ \frac{\left[1 - \left(\frac{M_1}{M_2}\right)^2 \sin^2\theta\right]^{1/2} + \left(\frac{M_1}{M_2}\right)\cos\theta}{1 + \left(\frac{M_1}{M_2}\right)} \right\}^2 , \quad (1)$$

where M_1 and M_2 are the mass of the projectile ion (usually He for RBS) and target atom, respectively. K is tabulated for various projectile ions, target atoms and scattering angles. A helium ion backscattering from a heavy atom will scatter with a greater energy than one scattering from a lighter atom. It is in this way that the target species can be identified.

In addition to helium ions which scatter off the atoms on the surface of the target, helium ions are also detected from scattering events in the bulk to a maximum depth of several thousand angstroms, depending on the ion energy and the target material. Helium ions that backscatter from atoms below the surface of the target will be detected with increasingly lower energies with greater depths, due to the loss of energy traversing the material, dE/dx. Therefore, the thickness of an elemental film is directly related to the width of its backscattering spectrum peak. The thickness of a thin film can be calculated from the energy width of the peak by[4]

$$t = \frac{\Delta E_{peak}}{N[\varepsilon]} , \quad (2)$$

where ΔE is the width of the peak in the natural unit of energy, $[\varepsilon]$ is the stopping cross section factor which is a function of the scattering angle and the stopping cross sections, ε, which are dependent on the ion energy and the material and are empirically known and tabulated, and N is the atomic density of the material. The thickness of a very thin film can also be calculated by[4]

$$t = \frac{A \cos\theta}{\sigma \Omega Q N} \quad , \tag{3}$$

where A is the total integrated number of counts under the spectrum peak, θ is the scattering angle, σ is the scattering cross section of the element, Ω is the solid angle of the detector, and Q is the total charge collected. Both methods yield nearly the same result for an elemental film. A sample target and its ideal RBS spectrum are shown below in Figure 3. Note that the Ti peak is shifted back from where its surface position would be since the Ti film is below the Al film. The C peak is also shifted from its surface position by the Ti and Al films.

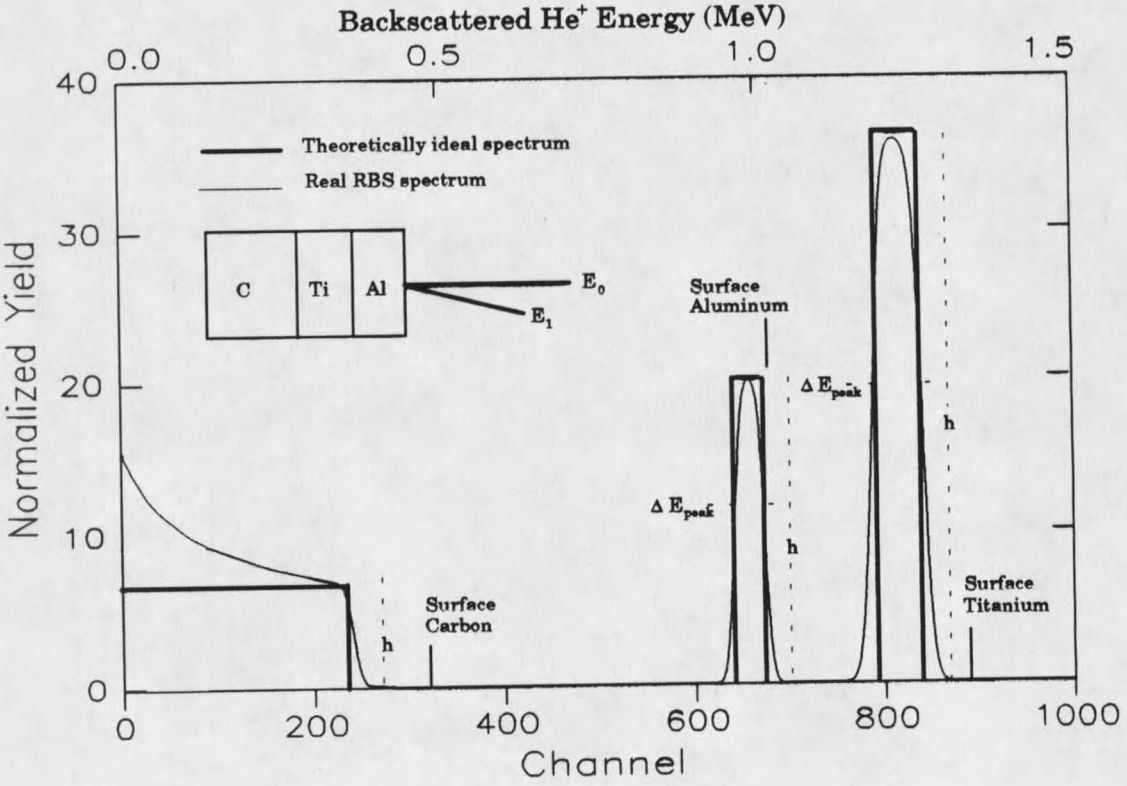


Figure 3. Sample target, real and ideal RBS spectra

As mentioned above, the energy width of the peak, ΔE_{peak}, shown in Figure 3 is directly proportional to the thickness of the elemental peaks. Likewise, the height of the peak is proportional to the mass of the element through σ, where

$$\sigma = \frac{1}{\Omega}\int_{\Omega}\left[\frac{Z_1 Z_2 e^2}{4E_c \sin^2(\theta_c/2)}\right]^2 d\Omega \qquad (4)$$

in the center of mass reference frame. Note that because σ is proportional to Z^2 of the target atom, the surface edge height of the peak is proportional to Z^2. Note also that the peak height of the carbon substrate goes as $1/E^2$ due to height ~ σ ~ $1/E^2$. Unfortunately, the reality of RBS spectroscopy is that elemental peaks do not have perfectly flat and smooth edges. This spreading out or rounding of the peaks has several origins. One is straggling, which is due to the random nature of an ion's energy loss as it travels through a solid. Another cause may be an incident beam that is not quite monoenergetic so that there is some greater spread in the scattering energy. Finally, there is some spreading of the signal due to the detector system resolution. It is usually convenient to represent these deviations by a Gaussian energy distribution. For the system used in this study, the system variance from all three contributions is around 24keV. It is important to be able to distinguish between the spreading due to the inherent resolution and the spreading that is caused by ion beam mixing as discussed in Chapter 4.

In the analysis of RBS data, the program RUMP[5], which is a program into which RBS spectra and parameters are input and then can be manipulated and analyzed, was used for actually calculating the film thicknesses by the formulae above and also for creating RBS simulations and comparing them with the collected data. The simulations provided a means of creating multilayered films of any given composition, generating a simulated RBS spectrum with the same experimental parameters, and

varying the thicknesses or compositions until the simulated and the real spectra match, again yielding and confirming information about film thickness and composition. Additionally, any impurities in the films could be identified and quantified from the RBS spectrum using RUMP.

Rutherford Backscattering analysis is also used in determining the amount of ion-beam induced mixing that occurred and whether there was specific compound formation. For an abrupt interface between elemental films, the corresponding edges (the back edge of the surface film and the front edge of the underlying film) on the RBS spectrum are also well defined, sharp, and have a steep slope. As the sample is mixed, interdiffusion between the two films occurs. This interdiffusion is evident in the RBS spectrum; the interface edges are not so sharp or steep, due to the surface atoms being pushed back into the underlying film and the atoms of the underlying film diffusing forward towards the surface. Quantification of the mixing based on the change in slope beyond the widening due to the inherent system resolution of the RBS spectrum peaks is discussed in the Results and Discussion Section.

Since the sample was characterized before and after mixing, it was exposed to air each time an RBS measurement was made. This led to the formation of an oxide layer on the surface of the sample which should not interfere with the mixing process. During the RBS spectra collection, the target was biased at +165V with respect to the chamber to trap secondary electrons which would otherwise leave the sample and erroneously increase the measured beam current.

Ion Beam Mixing

The apparatus used for the ion beam mixing is shown in Figure 4. It consists of 150 kV positive ion (argon) accelerator, a bending magnet and a chamber capable of

maintaining pressures below 2×10^{-8} Torr complete with a goniometer for mounting and manipulating the sample.

The ion beam mixing was done at base pressures below 5×10^{-8} Torr and during mixing the pressure was less than 3×10^{-7} Torr. The energy of the Ar^+ beam was chosen so that the range of the ions in the material was slightly greater than the depth of the interface of the Al and Ti. This range was calculated by means of TRIM (TRansport of Ions in Matter) computer code,[6] which calculates the range of an ion traveling in a solid based on the ion incident energy and scattering cross sections. The sample was aligned normal to the beam so that the beam (maximum ½ cm^2 area) was centered on the ½ inch diameter sample. The sample was biased at +165 V so that the current measured would be a true indication of the incident Ar^+ current. The total charge incident on the sample was monitored by a current indicator/integrator so that the dose (total incident particles per cm^2) could be calculated. The incident flux on the sample averaged around 10 $\mu A\ cm^{-2}$ so that the times of mixing ranged from 5 minutes for a dose of $2.5 \times 10^{15}\ cm^{-2}$ to 140 minutes for a dose of $7 \times 10^{16}\ cm^{-2}$. The temperature of the sample during mixing was monitored via a thermocouple and did not show any rise above room temperature for a dose of $1 \times 10^{16}\ cm^{-2}$, so that thermal mixing of Al-Ti was considered a negligible effect in the ion beam mixing process.

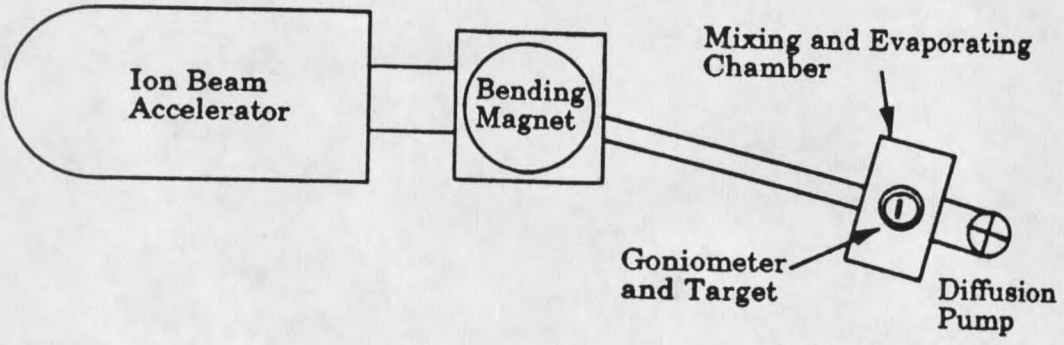


Figure 4. Schematic of apparatus used for ion beam mixing

CHAPTER 3

SAMPLE PREPARATION

The Ti and Al thin films were evaporated onto a carbon plug with an extra smooth pyrolytic carbon coating. The carbon plugs were purchased from Ted Pella Inc. and are standard sample mounts for scanning electron microscopy. Carbon was chosen for its reasonable heat capacity and because it would not interfere in the RBS analysis; being a lighter element, its RBS spectrum peak appears at a much lower energy than those of Al and Ti. Titanium was first evaporated onto the carbon plug by passing 3 to 5 A of current for 3 to 6 minutes through a 0.010" diameter 75/25 Ta/Ti alloy wire that is primarily manufactured for getter pumping Ti deposition for ultra high vacuum systems. Purity of the deposited Ti is guaranteed to be at least 99.5%.[7] The Ta/Ti alloy wire was approximately 6 inches in length and tightly coiled so that the bulk of the wire was directly in front of the graphite plug at a distance of ½ inch. The amount of resulting Ti deposition was approximately known based on the geometry of the evaporation setup and the yield of Ti from the Ta/Ti wire based on current and time. The base pressure was no greater than 2×10^{-8} Torr and rose to less than 3×10^{-7} Torr during evaporation. The aluminum was then evaporated on top of the Ti film by means of heating a tungsten basket holding Al wire (99.999% pure). The pressure during the Al evaporation did not go above 2×10^{-7} Torr. The time of Al deposition ranged between 5 and 10 minutes and the thickness was roughly monitored by visually observing the sample color change from the darker Ti layer to the lighter Al. Both the Ti and the Al films were fabricated in the same vacuum chamber so that the interface was not exposed to air. This minimized the contamination of the elemental films at the

interface due to oxygen, hydrogen, etc. The actual deposited thicknesses were obtained by RBS analysis as discussed in the analysis and experimental techniques section.

Initially, Ti deposition was attempted in the same manner as the Al, that is, by placing Ti foil pieces in a Tungsten basket and heating the basket. However, at the extremely high temperatures needed to melt the Ti, small amounts of W were also deposited with the film and there was some concern that the high temperature might induce some unwanted preliminary thermal interdiffusion of the Al and Ti. An attempt was also made to deposit Ti and Al by sputtering but this failed for several reasons, the most crucial being oxygen contamination due to the higher pressure in the chamber housing the sputter set-up and contamination of fluorine from the Teflon shielding of the home-made sputtering apparatus.

CHAPTER 4

THEORY

Mechanisms of Ion Beam Mixing

There are three basic mechanisms of ion beam mixing that have been identified. They are: ballistic or recoil cascade, thermal spike, and radiation enhanced diffusion, RED. Ballistic cascade mixing is perhaps the most intuitive of the mechanisms since it is easy to visualize the incoming ions colliding with the target atoms and causing them to recoil and collide with other atoms and so on. Most of these recoils are fairly low energy and result in small, randomly directed displacements of the atoms. These displacements are of course larger than the displacements due to thermal oscillations about the equilibrium point. It follows that the amount of mixing by this mechanism would be dependent on the masses of the constituent atoms, the atomic density of the material, the average minimum displacement energy of the atoms and the energy deposited by the impinging ion at the initial collision site. If the cascade is dense enough, a localized phase change (vaporization or melting) may occur. This is called a thermal spike. This mechanism is dominated by the thermodynamic properties of the materials (heats of formation and cohesion) as well as the density of the material and the energy deposited by the incoming ion. These two mechanisms are also called prompt processes since they occur after the first picosecond of each ion impact. Radiation enhanced diffusion is a delayed process since it occurs over a greater time than the prompt processes. It is diffusion of the atoms as a result of the mobility of vacancy and interstitial defects created by the initial ballistic or thermal spike cascade. RED is highly dependent on the temperature of the material; below the critical

temperature (which is somewhat below the temperature necessary for thermal diffusion for the material) the defect mobility is severely limited and RED is not a dominant effect. The resulting solid is not necessarily left in a state of thermodynamic equilibrium, due to the unusual nature of these mixing processes.

Quantifying the Amount of Mixing

Rutherford Backscattering Spectrometry (RBS) is the primary tool for quantifying ion beam mixing, as described in the analysis and experimental techniques section. When the concentrations of the elements vary monotonically across the interface, the amount of mixing is characterized by the variance which is a measure of the spreading of the peaks of the elements undergoing mixing. The mixing, or spreading, as a function of depth in the sample is best characterized by an error function with argument $(x-a)/\sqrt{4Dt}$ [8] , where Dt is the square of the effective diffusion length.[9] The variance, σ^2 , is then equal to 4Dt and has been shown to vary linearly with the dose[8] . In other words, the amount of mixing is directly proportional to the dose. Converting the RBS spectrum from count versus energy to counts versus depth for error function fitting is no simple task, so the variance can also be calculated by taking the square of one-half the difference between the energies, ΔE, at the positions of 84% and 16% of full height of the spectrum peak,[4] as shown in Figure 5. This energy squared is then converted into a depth squared by dividing it by the square of the energy loss factor, $(N[\varepsilon])^2$. Note that this energy loss factor is an average value for the interface calculated for a 50/50 composition of the elements assuming the Bragg Rule for 50/50 compounds ($[\varepsilon]_{ave} = \frac{1}{2}[\varepsilon]_A + \frac{1}{2}[\varepsilon]_B$, and $N_{ave} = \frac{1}{2} N_A + \frac{1}{2} N_B$).[4] The variance is calculated at various mixing doses for both elements, in this case, Al and Ti, and plotted for each element as a function of dose, ϕ. This data is then fitted to a

straight line by a least-squares fitting routine and the slope d(4Dt)/dϕ extracted. The quantity d(4Dt)/dϕ is defined as the mixing rate and is a standard way of quantifying mixing.

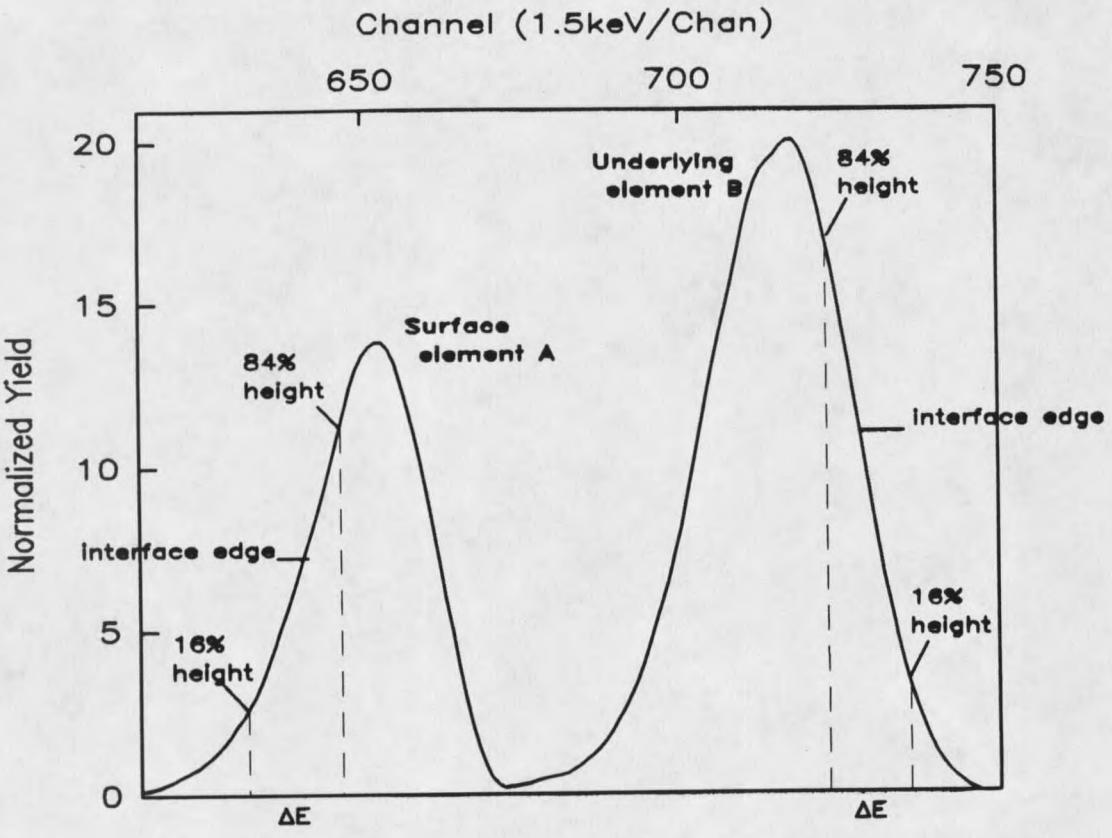


Figure 5. Finding ΔE for calculating the variance from the RBS spectrum

Models of Mixing Mechanisms

Currently, there are a few models that predict the mixing rate for various systems based on different thermodynamic considerations and favored mixing

mechanisms. It is suggested and shown for a few cases,[10] that systems which favor mixing by binary collision cascade can be modeled by[10,11]

$$\frac{d(4Dt)}{d\phi} = \frac{2}{3}\Gamma_0 \xi \frac{\varepsilon R_c^2}{NE_d} \quad , \tag{5}$$

where $\Gamma_0 = .608$, $\xi = [4m_1m_2/(m_1 + m_2)^2]^{1/2}$, ε is the energy deposited per unit path length at the interface, R_c is the mean-square range of a displaced atom, somewhat arbitrarily taken to be 10 Å, N is the average atomic density of the matrix, and E_d is the average minimum displacement energy for an atom in the target. For mixing dominated by the thermal spike mechanism, the mixing is modeled by[10,12]

$$\frac{d(4Dt)}{d\phi} = \frac{\varepsilon^2 K_1}{N^{\frac{1}{3}}(\Delta H_{coh})^2}\left[1 + K_2 \frac{\Delta H_{mix}}{\Delta H_{coh}}\right] \quad , \tag{6}$$

where ΔH_{coh} and ΔH_{mix} are cohesive energy and heat of mixing, respectively, and K_1 and K_2 are fitting constants, with K_1 found to be near 0.037 Å and $K_2 = 27$.[12] This model has also had some success for certain systems.[8,10,12,14] It has been suggested that for systems with an average atomic number less than 20, the mixing process should be dominated by binary collisions and therefore agree with equation (5) and that thermal spike mixing modeled by equation (6) will dominate for systems with an average atomic number greater than 20.[10] Since it is known that the mixing rate increases with the mass of the mixing ion,[13] it is not clear whether this relation between average atomic number and favored mixing process will be true for ion beam mixing with Ar^+ as well as Xe^+ for which it has been demonstrated.[10] It is also somewhat unclear whether the two models given above are adequate to represent bilayer mixing for Ar^+ mixing. These are some of the questions this work can help to resolve.

Thermodynamic Considerations

Also of interest in the mixing process is the role of the solubilities of the bilayer elements into each other. If small amounts of element A are soluble in B and small amounts of B are less soluble in A, should we expect A to diffuse into B from ion beam mixing as a rule? For this particular case, the approximate solubility obtained from a metallurgical phase diagram for Al in Ti at room temperature is nearly 10%, whereas Ti is not soluble in Al at room temperature to any measurable degree.[15] However, for ion beam mixing, it is not clear whether the relative solubilities of the elements assists, impedes or is irrelevant to the mixing process. If, in this case, small amounts of Al are soluble in bulk Ti and small amounts of Ti are not soluble in bulk Al, we might expect to see Al diffusing into the bulk of Ti and not vice versa.

There is also the consideration of whether ion beam mixing produced phase formation is favorable or even possible, and whether it might be predicted or explained based on thermodynamics. It has been shown that only the $TiAl_3$ phase is formed during thermal annealing of an Al-Ti bilayer.[16] Again, it is not clear that this disposition to form the $TiAl_3$ phase for thermal annealing plays a role in predicting phase formation in the ion beam mixed sample. The heats of formation for the three phases commonly formed are as shown in Table 1.[17] Thermodynamics would indicate that the favorable phase to form should be the 50/50 Al-Ti compound since its heat of formation is the largest. This γ-phase Al-Ti also has the simplest crystal structure: face-centered tetragonal structure that is very close to the face-centered cubic structure of Al. It has been suggested that phase formation due to ion beam mixing is more favorable for simple crystal structures and that there is no identifiable correspondence between the phase formed by thermal annealing and the phase formed by ion beam mixing.[18,19]

Phase formation	$\Delta H_{formation}$
$TiAl_3$	-36.6 kJ/g-atom
γ Al Ti	-37.4 kJ/g-atom
α_2 Al Ti_3	-24.6 kJ/g-atom

Table 1. Heats of formation for Al-Ti phases

CHAPTER 5

RESULTS AND ANALYSIS

Sample Analysis and Normalization

The as-deposited samples were first analyzed by RBS for composition, purity and film thickness. The RBS spectrum for an unmixed sample is shown in Figure 6. The average thickness of the Al film was calculated by RUMP and found to be 525Å with an assumed oxide (Al_2O_3) layer of 50Å. The thickness of the Ti film was calculated to be 400Å. It is apparent from Figure 6 that the interface edges of the Al and Ti are not as sharp as the ideal simulated spectrum.

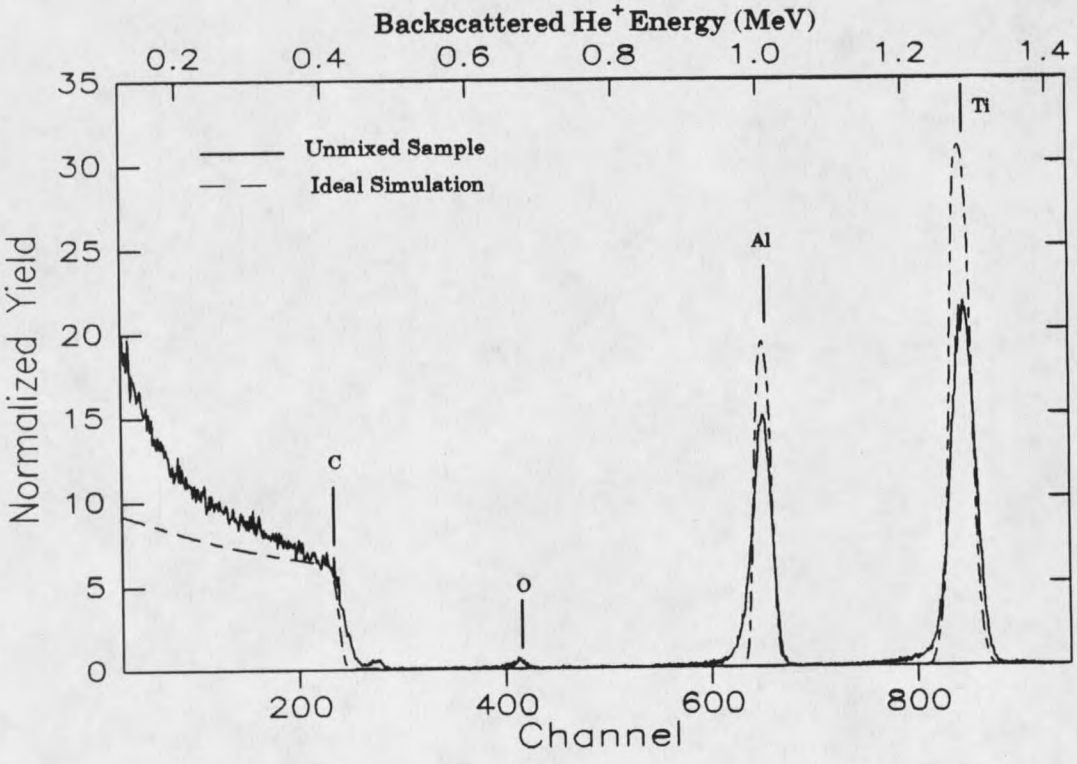


Figure 6. RBS spectrum of unmixed sample and ideal simulation

Since the simulation accounts for straggling and the detector resolution, the additional "fuzzing" at the interface is probably due to some initial natural interdiffusion between the Al and Ti. The possibility of interdiffusion due to heating during the evaporation process is unlikely since the temperature of the sample did not exceed 40°C above room temperature during the Ti deposition and 15°C for the Al evaporation as monitored by a chromel-alumel thermocouple.

The thickness and composition of the pre-mixing diffusion region were approximated by matching the raw RBS data with a simulated spectrum with RUMP as shown in Figure 7.

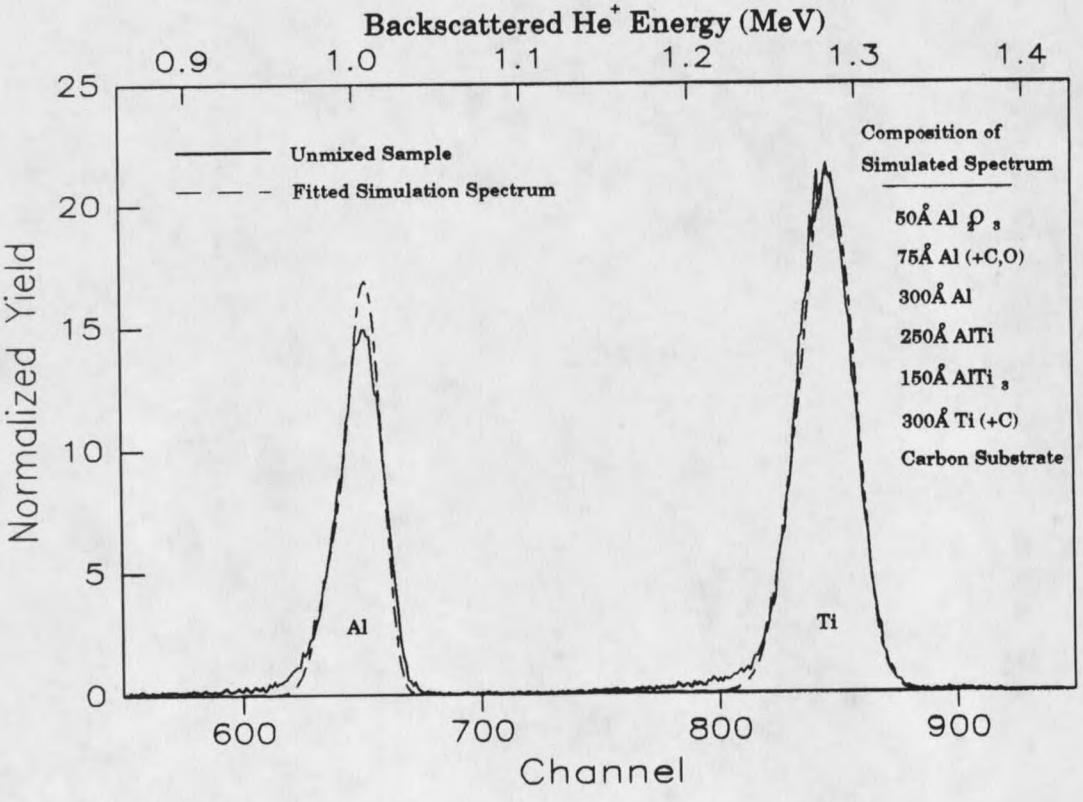


Figure 7. RBS spectrum of unmixed sample and fitted simulation

The composition of the unmixed sample was found to be nearly 250Å of AlTi on 150Å of $AlTi_3$ sandwiched between the pure Al and Ti layers. There is some uncertainty in these simulated thicknesses on the order of 50Å, mostly due to uncertainties in the parameters (charge, detector resolution, Bohr straggling, etc.) which RUMP uses to create the simulations and partly due to the somewhat arbitrary manner in which the user creates and modifies the composition of the simulation spectrum based on visually fitting the simulation to the raw data spectrum. The mechanism and composition of spontaneous diffusion at room temperature of Al and Ti is best left to other methods of analysis. In this study it is sufficient to note that since mixing (actually the variance) is a linear function of dose, any initial interdiffusion will not affect subsequent changes in variance as a function of dose. The best way to normalize the non-zero variance for zero dose is to subtract the initial mixing amount from that for the subsequent mixed data.

After the initial evaporation and each successive dose of ion beam mixing, the sample was analyzed by RBS. Two different spots on the mixed portion of the sample were analyzed to average out any great non-uniformity in the mixing ion beam and original sample composition. The raw spectral data was then smoothed by a 3-point, non-weighted averaging scheme to eliminate any rough places on the spectrum due to the nature of the backscattering events in the data collection. The change in energy from 84% to 16% of spectrum peak height on the interface side of both Al and Ti for each dose is then extracted as shown in Figure 8. The average energy loss factor over the interface region, $N[\varepsilon]$, is calculated once for each sample using approximate energies at the interface obtained from the data for an intermediate dose. Note that the tabulated values for ε vary not more than 5% for energy differences up to 200keV. Since the energies used to calculate ε at the interface vary less than 3keV from unmixed to the highest dose mixed sample, the value for $N[\varepsilon]$ will vary only slightly as the

sample is mixed, so the average value is more than adequate. The variance for each dose is then calculated, the variance for zero mixing subtracted, and the normalized variances plotted as a function of dose. The plot is then fitted with a least squares fit straight line as shown in Figure 9. The slope of the line is equal to $d(4Dt)/d\phi$, which is the mixing rate.

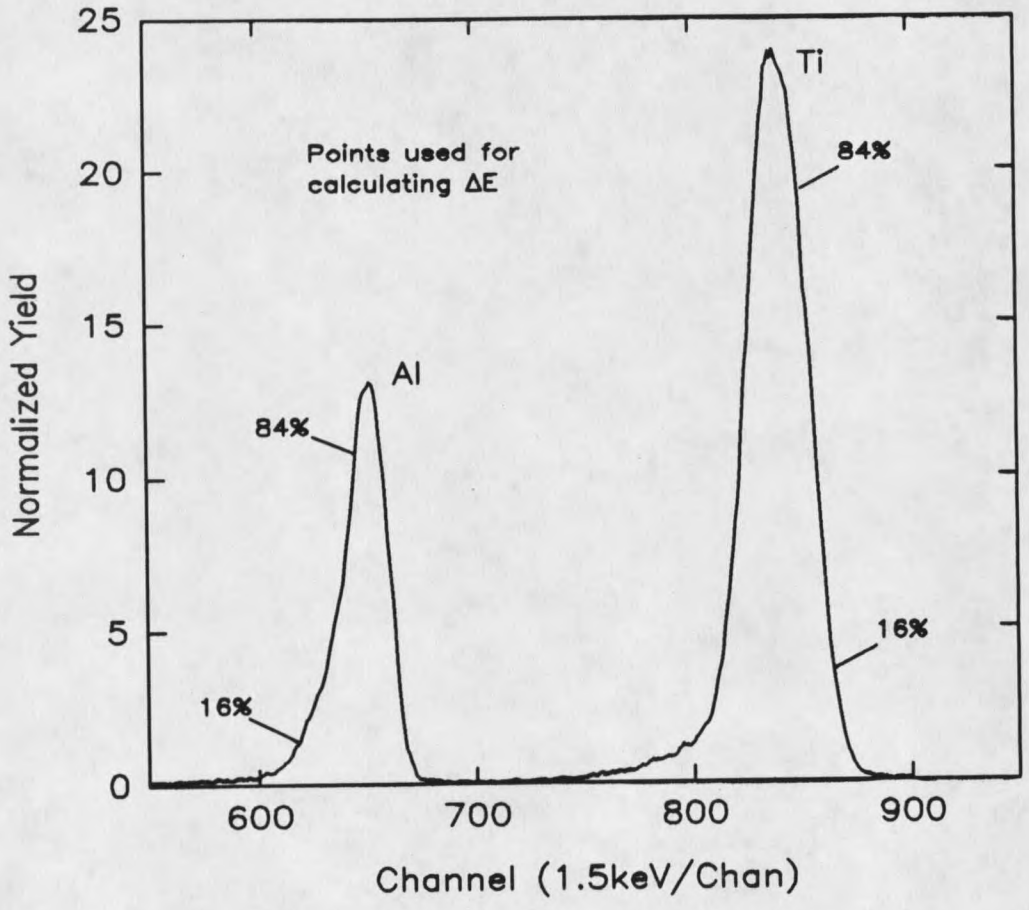


Figure 8. Demonstration of points used to find ΔE

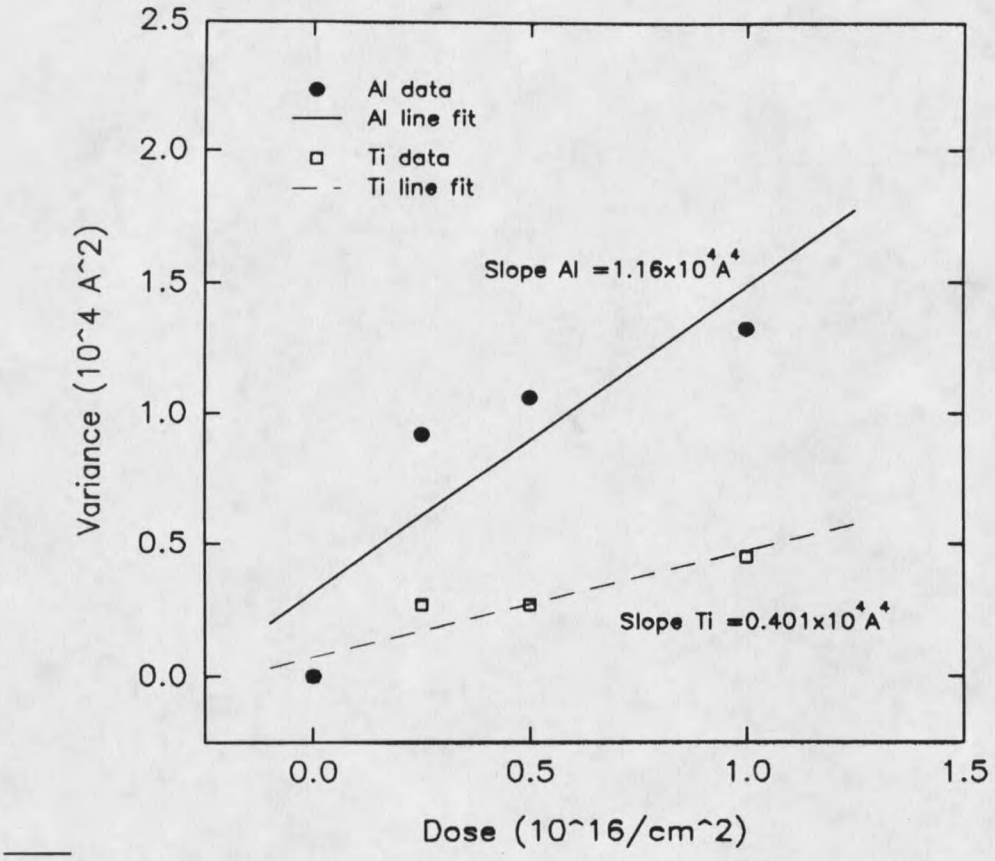


Figure 9. Plot of variance versus dose

Experimental Results

The experimental mixing rate obtained for this particular sample was found to be 1.16 (10^4Å^4) for the Al edge and 0.40 (10^4Å^4) for the Ti edge. Again, we do not necessarily expect the mixing rates to be the same for the Al and the Ti, even though they are adjacent to each other, due to variations in solubility or mobility. The average experimental mixing rate (½ of the mixing rate for Al edge plus ½ of the mixing rate for the Ti edge) for this sample is then 0.78 (10^4Å^4). Comparing these values of the mixing rates to the theoretical values based on the mixing models, it is assumed here

that the average of the mixing rates for the Al and Ti edge is used since neither model inherently distinguishes one edge from the other. The two models discussed here also do not distinguish between mixing by different ions, with the possible exception of the value for ε, the average energy deposited per unit length due to nuclear collisions at the interface which will certainly be greater for bombardment with the heavier Xe^+ than Ar^+. Note that the ballistic collision cascade model is proportional to ε, while the thermal spike model varies with ε^2.

The theoretical value obtained from the ballistic collision cascade model is

$$\frac{d(4Dt)}{d\phi} = \frac{2}{3}\Gamma_0 \xi \frac{\varepsilon R_c^2}{NE_d} = 0.23\ (10^4 Å^4) \qquad (7)$$

where the parameters are as previously defined, the value for E_d is taken to be 18eV[20] and ε is calculated by the TRIM computer code to be 61eV/Å for Ar^+ at the interface (with a nominal error of ±5eV/Å). The theoretical value of the mixing efficiency based on a thermal spike model is then

$$\frac{d(4Dt)}{d\phi} = \frac{\varepsilon^2 K_1}{N^{\frac{5}{3}} \Delta H_{coh}^2}\left[1 + K_2 \frac{\Delta H_{mix}}{\Delta H_{coh}}\right] = 0.28\ (10^4 Å^4) \qquad (8)$$

where , again, ε is 61eV/Å, ΔH_{mix}= -0.37eV/atom[13] and ΔH_{coh}= -4.49eV/atom.[21]

It is interesting that both models yield virtually the same result for Ar^+ mixing of Al-Ti. Since the average atomic number for Al-Ti is 17.5, mixing by the thermal spike mechanism should have been expected. This is indeed the case for Ti-Al mixing by Xe^+, where the experimental value of the mixing efficiency (assumed to be an average) was found to be 1.19 ($10^4 Å^4$) which corresponds to the ballistic mixing model which, for Xe^+ with ε equal to 262eV/Å, yields 0.98 ($10^4 Å^4$) and contrasts neatly with the thermal spike model which yields 5.56 ($10^4 Å^4$) for Xe^+ mixing,[10] showing that ion mixing of Al-Ti with Xe^+ is dominated by a ballistic mechanism.

Mixing Rates (10^4Å^4)			
Experimental Results		Ballistic Recoil Model	Thermal Spike Model
Al edge	1.16	—	—
Ti edge	0.401	—	—
Ar^+Average	0.781	0.24	0.28
Xe^+Average	1.19	0.98	5.56

Table 2. Experimental and modeled mixing rates of Al-Ti from Ar^+ and Xe^+ mixing

Γ_o	0.608	E_d	18eV
ξ	0.960	K_1	0.037Å
ε	61eV/Å	K_2	27
R_c	10Å	ΔH_{mix}	-0.37 eV/pt
N	0.0584 pt/Å^3	ΔH_{coh}	-4.49 eV/pt

Table 3. Table of parameters used to calculate the theoretical mixing rates for Al-Ti

Clearly for the case of ion mixing with Ar^+ neither the ballistic cascade model nor the thermal spike model is adequate to describe the mixing process since the experimental value is nearly three times the value predicted by either model. It is possible but unlikely that a systematic error in our measurements was a factor, such as the dose measurement being consistently off by a factor of three; the experimental value

would be closer to the predicted values but the preferred mode of mixing would still be indistinguishable since the models still predict similar values.

It is more likely that with further studies of metal bilayer mixing by Ar^+ that the thermal spike model could be adjusted for Ar^+ bombardment. One consideration would be to fit the parameter K_2 to the mixing data for several metal pairs (parameter K_1 depends on the bilayer materials and is assumed to be fairly constant for metal pairs)[8] , thereby allowing better agreement between experiment and theory. K_2 would have to be on the order of 100 as compared to the Xe^+ fitted value of 27 to improve the correlation. It is most likely that the theory is in need of modification since it has been shown previously that the mixing rate does not appear to vary with the square of ε for mixing by different ion species.[13]

It may be possible to describe the mixing process by another mechanism such as radiation-enhanced diffusion (RED). This, however, is unlikely since the critical temperature above which RED is likely to be dominant for Al-Ti is above 175 °C[22] and the thermocouple placed on the sample during the ion mixing detected no significant temperature increase.

It is important to note that despite the non-correlation between the experiment and the accepted models, that the experimental value obtained for the mixing efficiency by ion mixing Al-Ti bilayers with Ar^+, 0.781 (10^4Å^4) is less than the mixing efficiency of the same metal pair by Xe^+, 1.19 (10^4Å^4). This is in agreement with previous results that have shown that mixing rate increases systematically with the impinging ion mass.[13]

Phase Formation by Ion Beam Mixing

Thermal annealing of Al-Ti bilayers leads to $TiAl_3$ formation, but it is difficult in our case to determine if or to what extent phase formation occurred due to the limited

resolution of the RBS analysis for very thin films of Al-Ti phases and the initial spontaneous interdiffusion of the Al and Ti films. Figure 10 shows an RBS spectrum of $TiAl_3$ formation due to thermal annealing.[16] Note the plateaus formed due to the compound formation. Figure 11 shows the RBS spectra of the ion beam mixed sample at varying doses: unmixed, $0.5x10^{16}cm^{-2}$, and $2x10^{16}$.

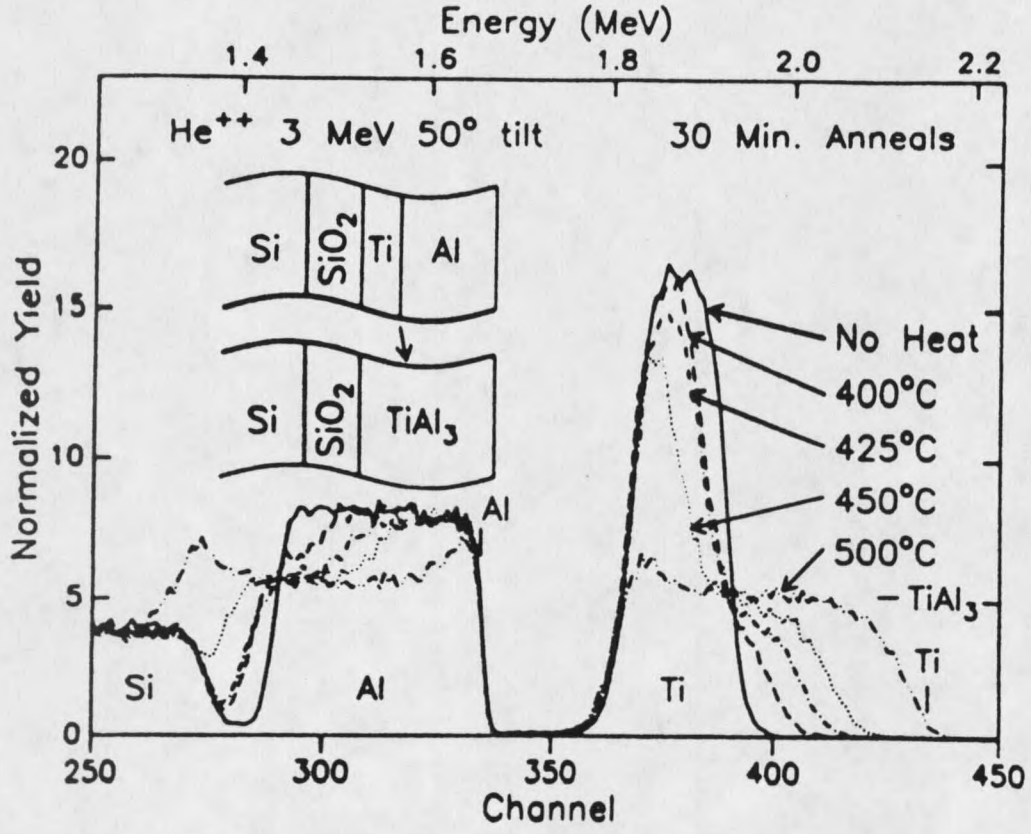


Figure 10. RBS spectrum of a thermally annealed Al-Ti bilayer (Ref. 16)

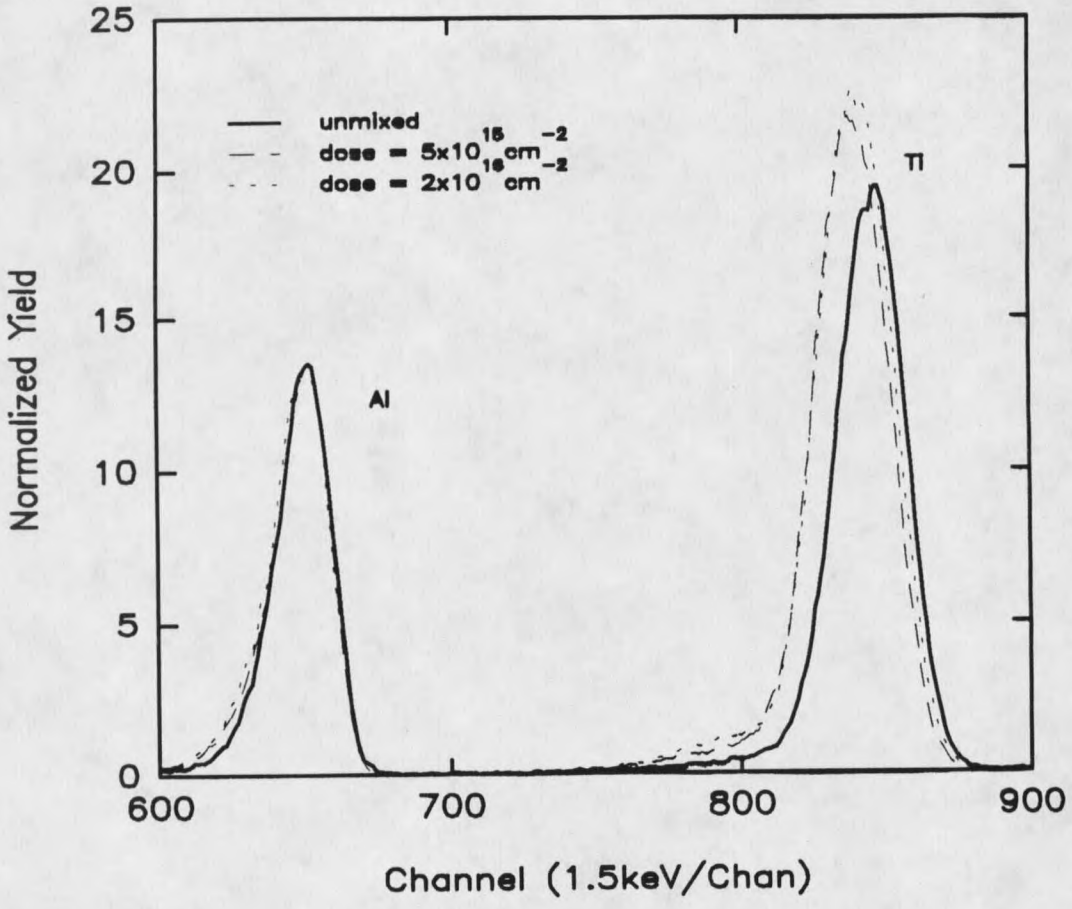


Figure 11. Overlay of the RBS spectra for various doses

Note that while the spreading of the elemental peaks due to mixing is evident, there are no obvious ledges formed due to compound formation. For comparison, a simulation of Al-Ti mixing with various compound formations is shown in Figure 12. The thicknesses of the simulated compound layers shown are 500Å to best display the features. A close examination and comparison of the mixed sample of Figure 13 to the phase simulations suggests that there may indeed be some phase formation.

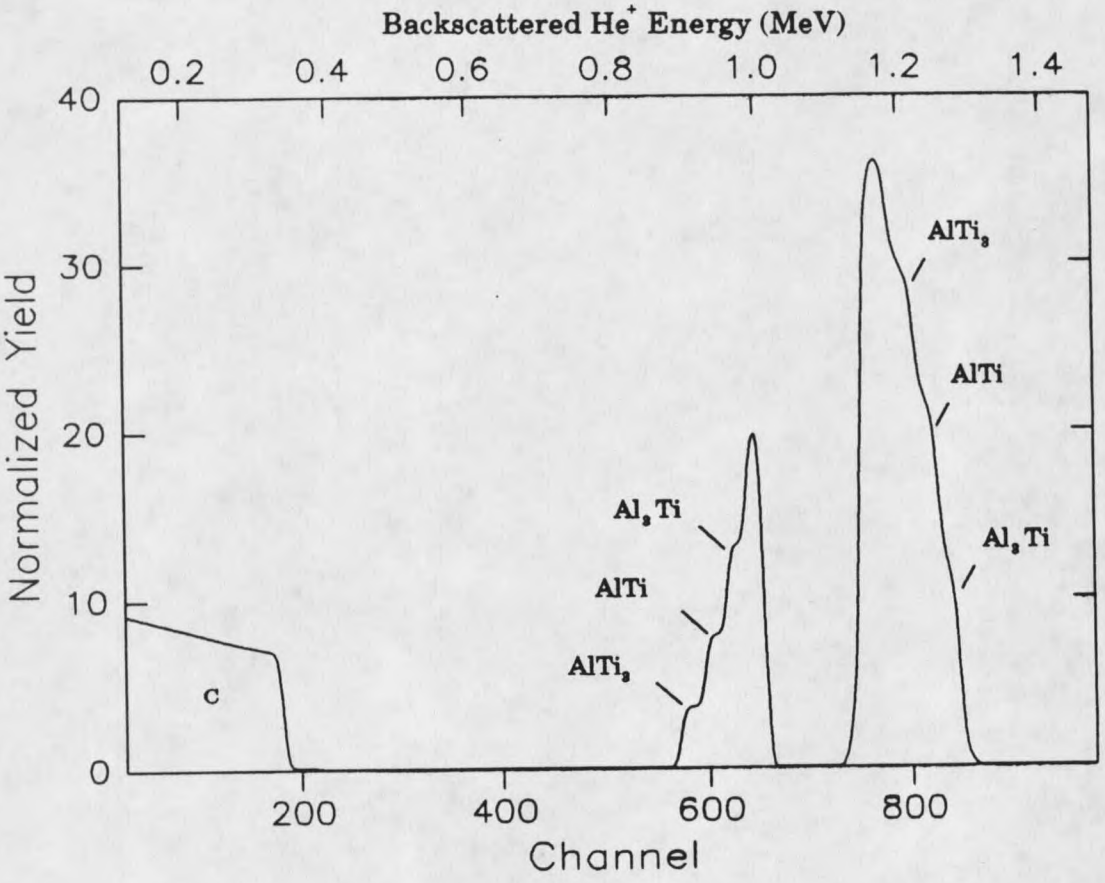


Figure 12. Simulation of the RBS spectra for the Al-Ti phases

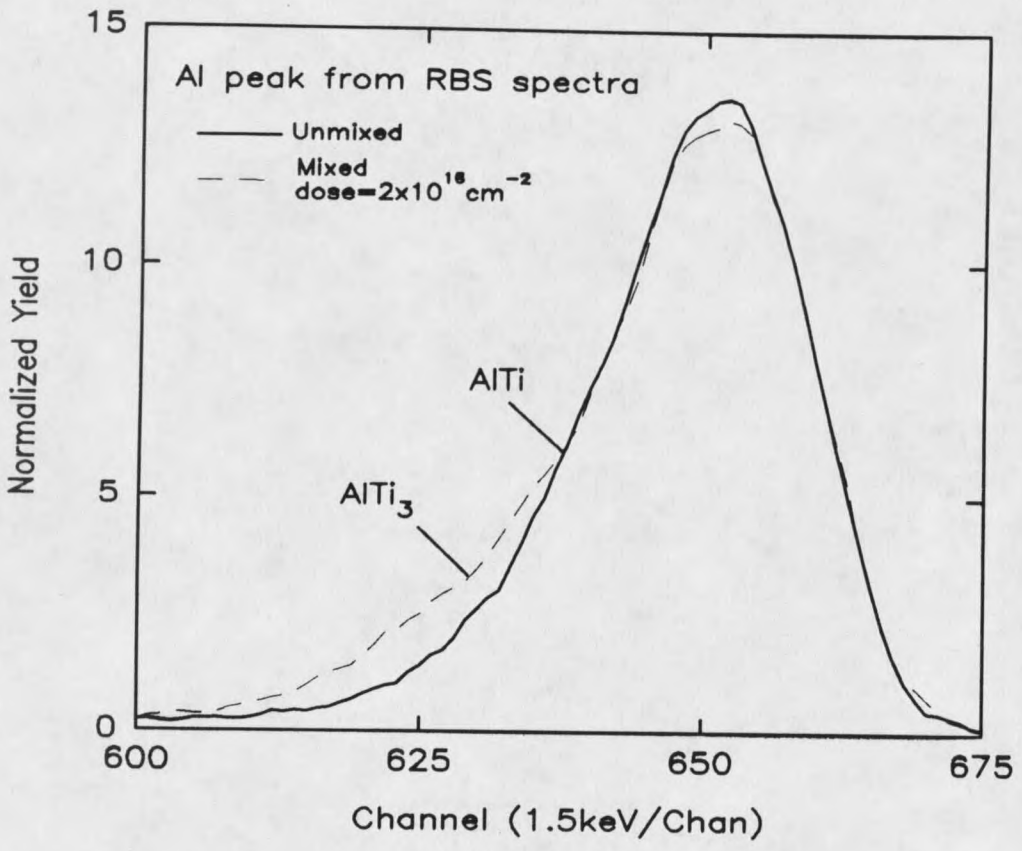


Figure 13. Enlargement of Al peak at two different doses to show possible phase formation

Figure 14 shows the same mixed sample and the corresponding fitted simulation. Note that the mixed regions are thicker than those of the unmixed sample, although they appear to have similar compositions. Even though the composition of the mixed region cannot be known exactly, it is *clear* that there is indeed mixing of the Al and Ti bilayer due to Ar^+ ion beam irradiation. From the data collected for this study it is inconclusive whether specific Al-Ti phases are or can be formed by ion beam mixing. What can be concluded is that the dominant moving species for this bilayer pair is the Aluminum. This is demonstrated best in Figures 11 and 13 of the mixed sample. Note that the back edge of the Al extends to a greater depth in comparison to the unmixed

sample. The compositions of the layers of the fitted simulation also indicate that Al has moved deeper into the sample with additional mixing. In contrast, the front edge of the Ti does not appear to move forward from its initial position.

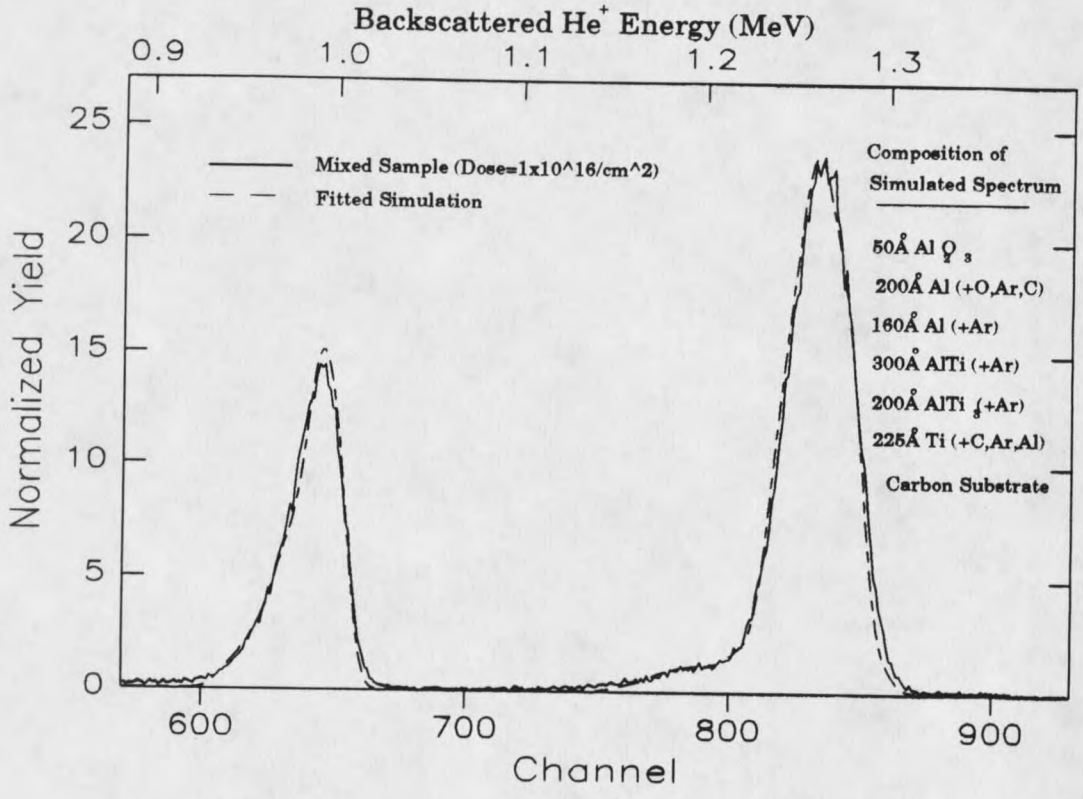


Figure 14. RBS spectrum of a mixed sample and fitted simulation

From this result it can be concluded that the species which is more soluble in the other is indeed the dominant diffusing species. In this case it appears that because Al is more soluble in Ti than Ti in Al, Al diffuses into the Ti and not vice versa. It is also interesting to note that as indicated before, the most thermodynamically favorable phase to form is the γ-phase AlTi. It may not be surprising, then, that this is one of the probable phases formed by ion mixing, but, the second most thermodynamically favorable phase to form is $TiAl_3$ and there was no indication of a tendency to form this

phase. However, the $TiAl_3$ phase is the phase formed from thermal annealing so it is quite puzzling that this phase does not seem to form in ion beam mixing. From this result it can be concluded, then, that the phase formed by thermal annealing does not indicate the phases formed or predict the moving species for ion beam mixing. It can also be concluded that the heat of formation is not the primary driving force in phase formation in ion beam mixing since the likely phases to have formed are not the two phases with the highest heats of formation. See Table 1 in the Theory section.

Discussion of an Earlier Sample

It should be noted here that an earlier sample similar in preparation and composition to the sample discussed above yielded some seemingly dissimilar results. Figure 15 shows the plot of variance versus dose for this sample. While the linear fit of the data is maybe not as aesthetically convincing, the average of the slopes (or mixing rates) of the Ti and Al edges is nearly the same as for the other sample at 0.75 ($10^4 Å^4$). It was initially unclear whether this result is coincidental or valid because not only are the mixing rates for the Al and Ti different from the previously discussed sample by a factor of two, but the mixing rate of Ti for this sample appears to be *larger* than the mixing rate of Al for the same sample. A plot of the RBS spectra taken after various doses for this sample is shown in Figure 16. The Al peak is much decreased in size due to sputtering at the relatively high dose. The back interface edge of the Al peak does not increase in slope as much as the interface edge on the Ti peak. This would seem to indicate that Ti is diffusing more readily into the Al than vice versa which is contrary to what was found in the originally discussed sample. If the variance versus dose is not truly linear, this seeming contradiction may be a result of the difference of the range over which the samples are mixed. This, however is unlikely since it has never been shown that variance does not increase linearly with dose.

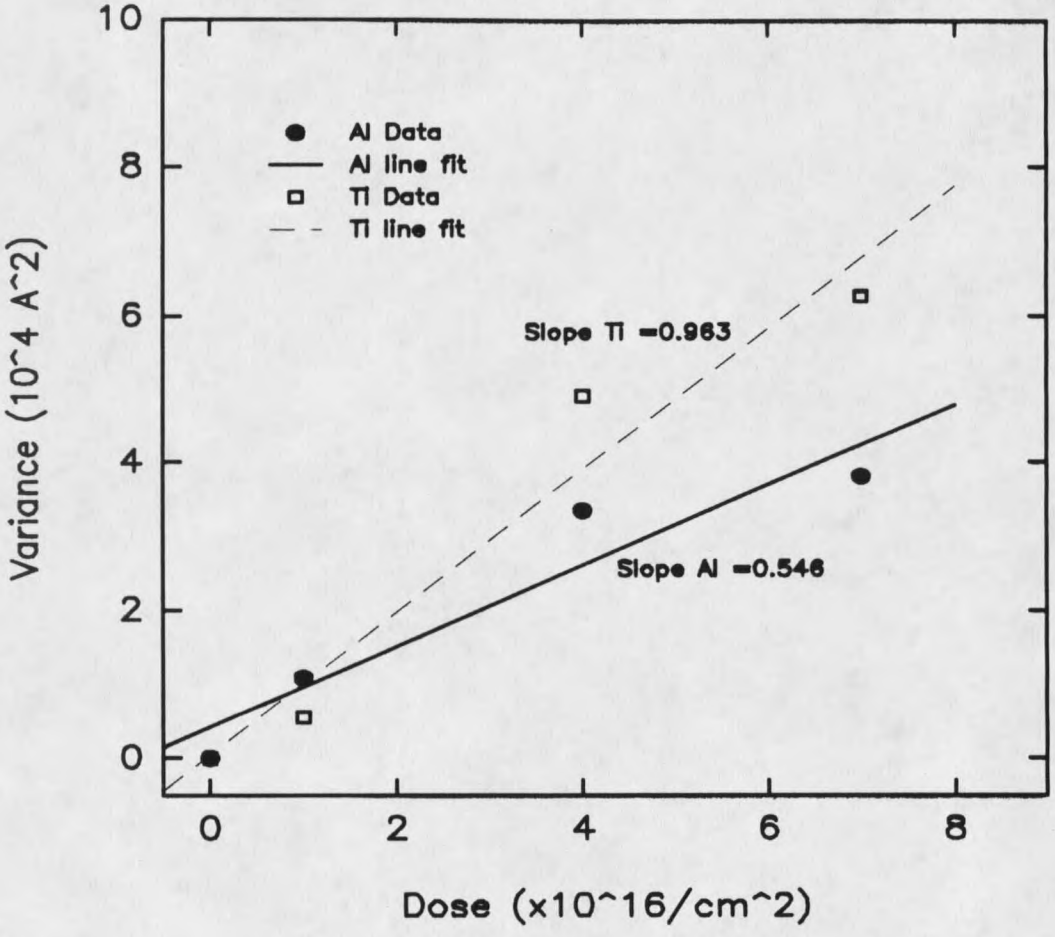


Figure 15. Plot of variance versus dose for a previous sample

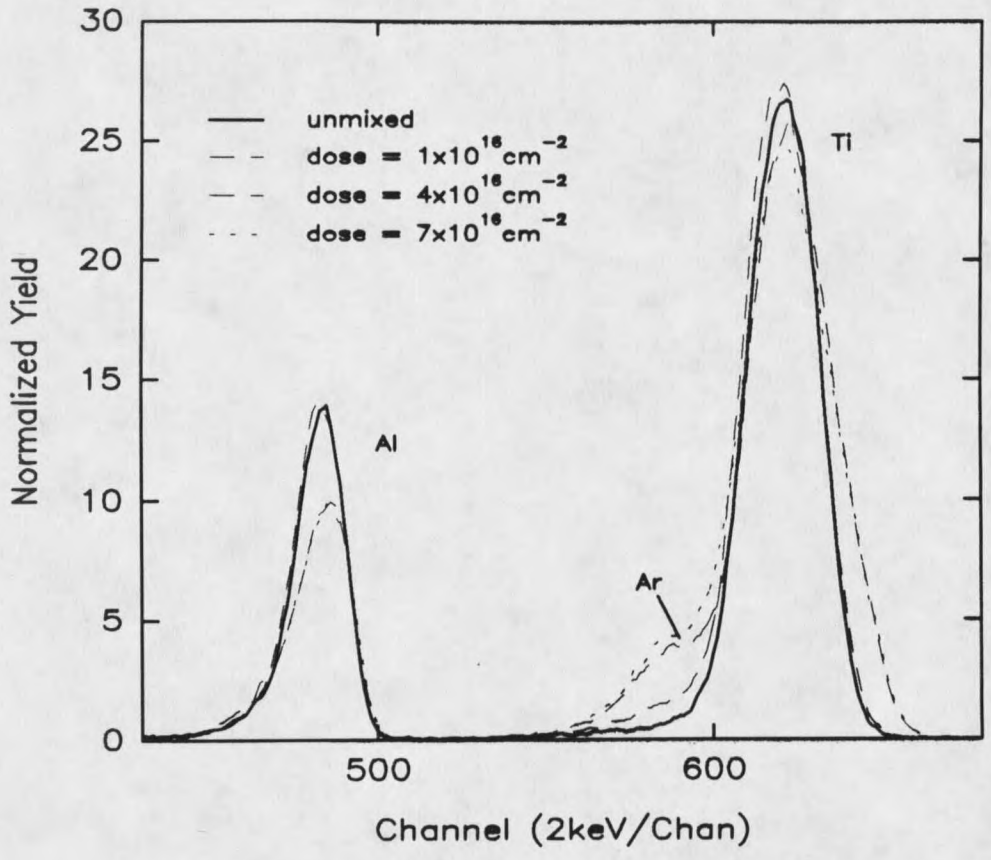


Figure 16. Overlay of the RBS spectra for various doses for a previous sample

What is more probable is that the amount of Al sputtered off the surface of the target over the higher doses affects the amount of Al that appears to move into the sample. Said another way, the Al sputtered off the surface of the sample at high doses changes the height and shape of its RBS spectrum peak by making the peak shorter and thinner. It is important in calculating the change in the variance over many doses that the reference part of the Al peak, i.e. the elementally pure Al layer, be invariant relative to the diffusion region over the different doses. This ensures that the measurement of the energy spread, ΔE, between the 84% and 16% heights is a true indication of widening of the layer, whereas the ΔE for a greatly sputtered peak would *decrease* due

to the shortening of the spectrum peak height. To be certain that the amount of Al on the surface is not decreasing significantly with dose, the total amount of Al can be calculated by integrating under the Al peak on the RBS spectrum and normalized by dividing out the charge and detector solid angle. The percentage change in Al peak area versus dose for each sample is shown in Table 4. Some amount of variation in the peak can be expected due to non-uniformities in the film thicknesses over the surface of the sample. It is clear that at the higher doses used on sample 2, a large and significant amount of Al was sputtered away, whereas the variations in the Al peak area of sample 1 are minimal (the apparent positive increases in Al peak area are due to small variations in film thickness over the sample and the difficulty of looking at the same location on the sample for each successive analysis). The changes in the area of the Ti peaks for both samples are small and show no trend with dose which was expected since the Ti layer is shielded by the Al layer.

Dose ($10^{16}cm^{-2}$)	Sample 2	Sample 1
0	0%	0%
0.25	—	+0.6%
0.5	—	+3%
1.0	-3%	+0.4%
2.0	—	+2%
4.0	-21%	—
7.0	-20%	—
12.5	-59%	—

Table 4. Percentage of Al sputtered away as a function of dose

The doses applied to this earlier sample are not as well defined since a modification to the set-up for dose measurement was made after its analysis. It is estimated that the actual dosages for this sample may be larger than the measured dosages by roughly a factor of two. This estimate is obtained by noting that the area of the discolored region of the sample where the mixing beam appeared to be striking the sample was about one-half of the area over which the ion beam was originally assumed to be striking. This is encouraging, since this factor of two in the dose would scale the mixing rate of the Ti to 0.482 (10^4Å^4) which is quite close to the previously discussed result of 0.401 (10^4Å^4) for the Ti interface. It can be concluded, then, that the variance in the Al distribution is a result of the significant change in the Al spectrum peak size due to sputtering. For thin films at these high doses where a large amount of sputtering occurs, greater care must be taken in interpreting the data.

CHAPTER 6

CONCLUSION

Thin films of Al and Ti were first evaporated on a carbon substrate and then ion beam mixed with a 65-75keV Ar^+ beam at varying doses. The motivation for this experiment was to find if a phase or phases of titanium aluminides could be formed by ion beam mixing. Phase formation to any significant degree was not observed in the ion mixed samples. Amorphous mixing of the Ti and Al, however, was observed. The variation of the elemental concentration across the mixed region can be analyzed by calculating the mixing rate which is a function of the spreading of the RBS spectral elemental peaks. The mixing rate can be characterized using different models, mixing due to the ballistic recoil mechanism and to the thermal spike mechanism by comparing the calculated mixing rate to the experimentally determined value. It was found, that for Ar^+ mixed Al-Ti, the calculated mixing rate for both the ballistic recoil mechanism and the thermal spike mechanism yielded nearly the same value which was significantly lower than the experimentally determined value. This led to the conclusion that the accepted models for the dominant mode of ion beam mixing, the ballistic recoil mechanism and the thermal spike mechanism which predict results nicely for ion mixing with Xe^+, do not adequately describe ion mixing with Ar^+. The results from ion mixing with Ar^+ were lower than those of ion mixing with Xe^+ which was expected since the amount of mixing scales with the mass of the impinging ion.

The dominant moving species in the ion mixing of Al-Ti bilayers was found to be Al. This was as expected since at room temperature Al is more soluble in Ti than Ti is in Al. By fitting the RBS spectra of the mixed samples it was found that the compounds formed were those rich in Ti or having equal amounts of Ti and Al. This

agrees with the solubilities of the two materials in each other. It is interesting that the phase formed by thermal annealing of Ti-Al bilayers is $TiAl_3$. It appears that the processes which determine phase formation by thermal annealing are not the same as those at work in ion beam mixing.

REFERENCES

1. F.H. Froes, C. Suryanarayana and D. Eliezer, ISIJ International Vol 31 (1991), No. 10

2. Materials and Technology flyer, American Physical Society

3. F.W. Saris, *Structure-Property Relationships in Surface-Modified Ceramics*, edited by C.J. McHargue et al., 103-116 (1989)

4. W.K. Chu, J.W. Mayer and M-A.Nicolet, *Backscattering Spectrometry* (Academic, Orlando, FL, 1978)

5. RUMP Rutherford Backscattering Analysis Package, Computer Graphics Services (1989)

6. TRIM Computer Program, From: *The Stopping and Range of Ions in Solids*, J.F. Ziegler, J.P. Biersack and U.L. Littmark (Pergamon Press 1985)

7. Getters Corporation of America

8. T.W. Workman, Y.T. Cheng, W.L.Johnson, and M-A. Nicolet, Appl. Phys. Lett. 50 (21), 25 May 1987

9. B.M. Paine, R.S. Averback, Nucl. Instr. and Meth. in Phys. Res.B7/8 (1985) 666- 675

10. E. Ma, T.W. Workman, W.L. Johnson, and M-A. Nicolet, Appl. Phys. Lett. 54(2), 30 January 1989

11. P. Sigmund and A. Gras-Marti, Nucl. Instr. and Meth. 182/183 (1981)25-41

12. W.L. Johnson, Y.T. Cheng, M. Van Rossum and M-A. Nicolet, Nucl. Instr. and Meth. in Phys. Res. B7/8 (1985) 657-665

13. P. Børgesen, D.A. Lilienfeld, and H.H. Johnson, Appl. Phys. Lett. 57 (14), 1 October 1990

14. P. Børgesen, R.E. Wistrom, and H.H. Johnson, J. Mater. Res., Vol. 4. No. 4, Jul/Aug 1989

15. *Constitution of Binary Alloys*, edited by M. Hansen (McGraw-Hill, New York, Toronto, London 1958)

16. E.G. Colgan and J.W. Mayer, J. Mater, Res., Vol. 4, No. 4, Jul/Aug 1989

17. *Selected Values of the Thermodynamic Properties of Binary Alloys*, edited by R. Hultgren, (American Society for Metals, Ohio 1973)

18. L.S. Hung, M. Nastasi, J. Gyulai, and J.W. Mayer, Appl. Phys. Letter. 42 (8), 15 April 1983

19. M. Nastasi, L.S. Hung, and J.W. Mayer, Appl. Phys. Letter. 43 (9), 1 November 1983

20. H.H. Andersen, Appl. Phys. 18, 131 140 (1979)

21. *Thermal Physics*, C. Kittel and H. Kroemer, (W.H. Freeman and Company, New York, 1980)

MONTANA STATE UNIVERSITY LIBRARIES
3 1762 10179129 9

HOUCHEN
BINDERY LTD
UTICA/OMAHA
NE.